Synthesis and evaluation of indazole based analog sensitive Akt inhibitors†‡

Tatsuya Okuzumi,[a] Gregory S. Ducker,[b] Chao Zhang,[a] Brian Aizenstein,[c] Randy Hoffman[c] and Kevan M. Shokat*[ab]

Received 5th March 2010, Accepted 19th April 2010
First published as an Advance Article on the web 28th June 2010
DOI: 10.1039/c003917a

The kinase Akt is a key signaling node in regulating cellular growth and survival. It is implicated in cancer by mutation and its role in the downstream transmission of aberrant PI3K signaling. For these reasons, Akt has become an increasingly important target of drug development efforts and several inhibitors are now reaching clinical trials. Paradoxically it has been observed that active site kinase inhibitors of Akt lead to hyperphosphorylation of Akt itself. To investigate this phenomenon we here describe the application of a chemical genetics strategy that replaces native Akt with a mutant version containing an active site substitution that allows for the binding of an engineered inhibitor. This analog sensitive strategy allows for the selective inhibition of a single kinase. In order to create the inhibitor selective for the analog sensitive kinase, a diversity of synthetic approaches was required, finally resulting in the compound PrINZ, a 7-substiututed version of the Abbott Labs Akt inhibitor A-443654.

Introduction

The serine/threonine kinase Akt (PKB) is a signaling node in many cellular processes including cell growth and survival. It is a key downstream effector of phosphoinositide 3-kinase (PI3K) and sends signals to a wide range of apoptotic and metabolic regulators including GSK3, FOXO and TSC2.[1] Because the PI3K/Akt signaling pathway is dysregulated in a number of human diseases such as cancer and diabetes, modulation of the pathway is a significant therapeutic goal. Three Akt inhibitors have now advanced into late stage development or early clinical trials: MK-2206 (Merck),[2] GSK-690693 (GlaxoSmithKline),[3] and A-674563 (Abbott).[4] As a result of the large size of the human kinome and the close structural relationship between kinases, small molecule inhibitors of kinases are rarely perfectly selective for their intended targets and often inhibit other related kinases as well. To address the challenge of specific kinase inhibition we have developed an approach which exploits the power of genetics to sensitize a single kinase to inhibition by a pyrazolopyrimidine based series of inhbitors. We have termed this approach chemical genetics and applied it to over 40 different protein kinases.[5–9] In attempting to apply the approach to Akt we realized that the pyrazolopyrimidine based scaffold was not optimal for potent and selective inhibition of each Akt isoform. Here, we describe the development of a class of indazole based chemical genetic inhibitors against each isoform of Akt to overcome this limitation.

Mammalian cells contain three genes that encode three closely related and highly conserved isoforms of Akt, termed Akt1/2/3. Mouse knockout studies have uncovered distinct physiological functions for the three Akt isoforms: Akt1-deficient mice display developmental defects, Akt2-deficient mice have defects in glucose homeostasis, and Akt3-deficient mice show defects in neuronal development.[10] Akt1 has also been shown to be required for ErbB2 induced mammary oncogenesis and governs breast cancer progression *in vivo*.[11] The development of isoform selective Akt inhibitors will ultimately allow dissection of the complex biology controlled by each of these critical kinases.

Abbott labs reported the first selective Akt inhibitors based on an indazole scaffold (Fig. 1a). Our own profiling of this compound against a panel of protein kinases revealed this inhibitor also inhibits a wide variety of kinases closely related to Akt. Similarly, GSK reported GSK690693 as an ATP competitive Akt inhibitor.[3] In contrast to the ATP competitive inhibitors A-443654 and GSK690693, the Merck Akt inhibitor series based on a quinoxaline scaffold binds outside of the ATP binding pocket and exhibits unusual Akt selectivity compared to other kinases.[12] Merck has further refined this compound to obtain MK-2206, which is now being tested in clinical trials.[2] These compounds show a remarkable ability to inhibit subsets of Akt isoforms, but absolute isoform specificity remains elusive.

We have recently reported strikingly different cellular responses to ATP competitive Akt inhibitors compared to the non-ATP site class of inhibitors.[13] Our group and others

[a] *Howard Hughes Medical Institute and Department of Cellular and Molecular Pharmacology, University of California, San Francisco, 600 16th Street, MC 2280, San Francisco, California 94158, USA. E-mail: shokat@cmp.ucsf.edu; Fax: +1-415-514-0822; Tel: +1-415-514-0472*
[b] *Department of Chemistry, University of California, Berkeley, Berkeley, CA 94720, USA*
[c] *SelectScreen Services, Discovery Assays and Services, Cell Systems Division, Life Technologies Corporation, Madison, Wisconsin, USA*
† Electronic supplementary information (ESI) available: Supplementary Table 1. See DOI: 10.1039/c003917a
‡ This article is part of a *Molecular BioSystems* themed issue on Chemical Genomics.

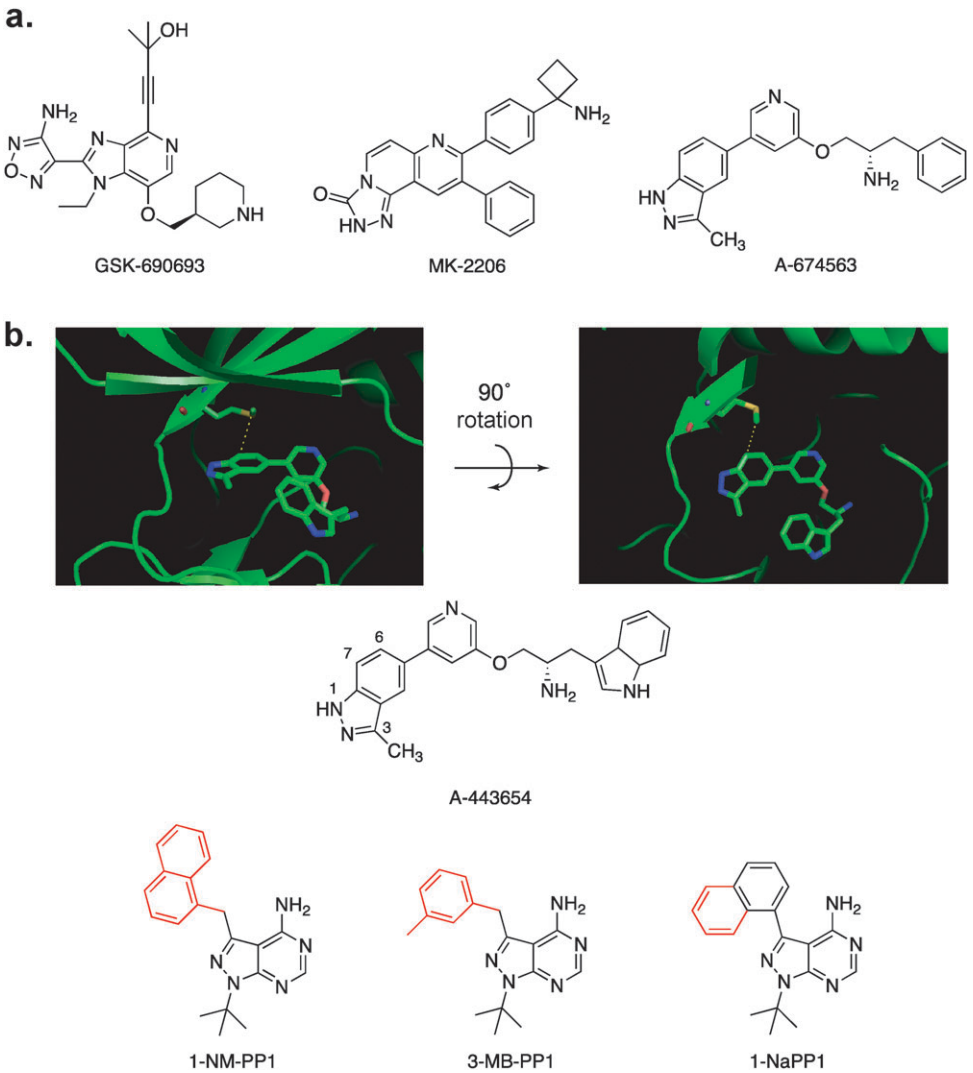

Fig. 1 (a) Structures of disclosed Akt inhibitors in clinical development. (b) Analog sensitive design strategy. Crystal structure of Akt2 with A443654 shows the native gatekeeper methionine and its proximity to the 7 position of indazole ring. Structures of PP1 derivatives commonly used to inhibit analog sensitive kinases.

have observed that ATP competitive inhibitors induce a striking and counterintuitive hyperphosphorylation of Akt itself.[14] To investigate this paradoxical result we required a highly selective ATP competitive Akt inhibitor to perform a mechanistic analysis of this unusual signaling effect. Thus we decided to employ a chemical genetics strategy using Akt isoforms that have been engineered to enlarge the ATP pocket, resulting in sensitization to inactive derivatives of kinase inhibitors.[15] This approach exploits a conserved, large hydrophobic residue in the kinase active site (termed the gatekeeper), which is in direct contact with the N6 amino group of ATP. By mutating the gatekeeper residue to a small residue such as glycine or alanine, mutant kinases have been engineered to accept inhibitors that cannot interact with the wild-type (*wt*) counterpart (Fig. 1b). Knocking-in an *as*-kinase (analog-sensitive) by substituting for the endogenous *wt* kinase in cells or organisms followed by treatment with an *as*-kinase specific inhibitor allows for the real-time pharmacological investigation of the role of a single kinase.[16] In addition to the use of pyrazolopyrimidine1 (PP1) analogues, a versatile starting point for the development of many analog sensitive kinase inhibitors,[6,17] we report here the development of inhibitors based on a completely different scaffold, that of the Abbott Akt inhibitor, A-443654.[18] These molecules are more potent against Akt-*as* isoforms than PP1 analogues either *in vitro* or *in vivo* without disrupting Akt-*wt* and will allow for the detailed investigation of the role of individual Akt isoforms in normal and disease physiology.

Results and discussion

Chemical synthesis

A-443654 analogues with bulky substituents at the C-7 position predicted to be oriented toward the Akt gatekeeper residue (M227 in Akt1, M225 in Akt2, and M229 in Akt3) were synthesized by Stille coupling of stannyl pyridine **Y2**[18] with bromoindazole **Y1** substituted at the C7 position

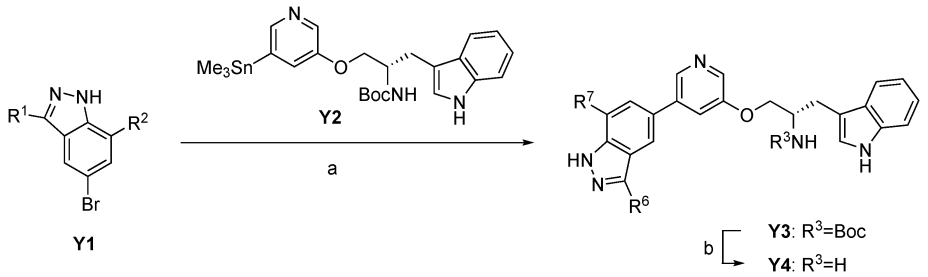

Scheme 1 (a) $Pd_2(dba)_2$, P(*o*-tol)$_3$, Et_3N, DMF, 90 °C, over night, (b) TFA, CH_2Cl_2, rt, 1 h, yield: 8–29% for 2 steps.

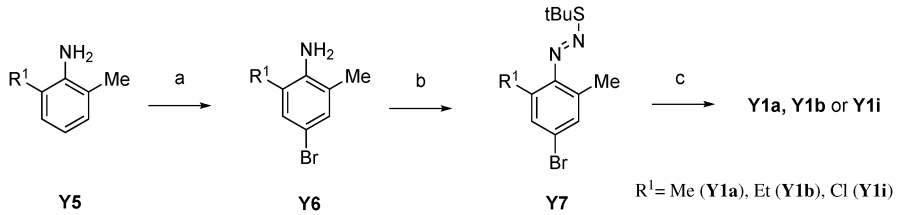

Scheme 2 (a) Br_2, AcOH, 0 °C, 2.5 h, yield: 88% for **Y5b**, (b) $NaNO_2$, HCl, H_2O, −20 °C, 30 min then *t*BuSH, 0 °C, 1 h, (c) *t*BuOK, DMSO, rt, over night, yield: 54–71% for 2 steps.

followed by deprotection of the Boc group on the tryptophanol moiety[18] (Scheme 1). Syntheses of bromoindazole building blocks (**Y1a**, **Y1b** and **Y1i**) is described in Scheme 2. Commercially available 2-alkyl-4-bromo-6-methylanilines (in the case of **Y6a** and **Y6i**), which can be prepared by bromination of commercially available 2-alkyl-6-methylaniline (in a case of **Y5b**), were diazotized and quenched with *t*-butylthiol to give diazosulfides (**Y7**). Basic treatment of **Y7** lead to an intramolecular cyclization affording bromoindazole intermediate **Y1**.[19] However, due to poor commercial availability of **Y5** and **Y6**, a procedure to introduce an alkyl group at the C7 position on indazole ring was required.

We next attempted a direct substitution of the chloride group on the indazole ring of **Y3i** with an alkyl group by Suzuki coupling using alkylboronic acid under Hartwig palladium catalyst conditions[20] (Scheme 3). Treatment of **Y3i** with *n*-butylboronic acid in presence of $Pd(dba)_2$ and Q-phos followed by deprotection of Boc group afforded the desired **Y4d** with 2% yield. Although the simplicity of this route makes it an attractive alternative for derivatizing the C7 position, because of the low yield, we decided to introduce the C7 substituent prior to the Stille coupling.

We thus used Suzuki coupling of 2-bromo-6-methylaniline with vinylboronic acids to prepare C7-alkylsubstituted bromoindazole building blocks (Scheme 4). Suzuki coupling of vinylboronic acids with 2-bromo-6-methylaniline (**Y8**) followed by hydrogenation of the double-bond to give

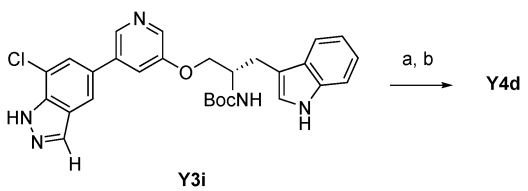

Scheme 3 (a) *n*BuB(OH)$_2$, $Pd(dba)_2$, K_3PO_4, Q-Phos, toluene, 90 °C, over night, (b) TFA, CH_2Cl_2, rt, 1 h, yield: 2% for 2 steps.

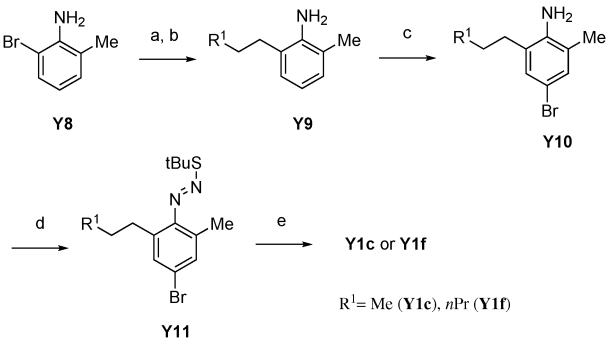

Scheme 4 (a) $R^1CH{=}CHB(OH)_2$, $Pd(PPh_3)_4$, Na_2CO_3, DME, 85 °C, over night, (b) H_2, Pd/C, EtOH, rt, over night, yield: 62–76% for 2 steps, (c) Br_2, AcOH, 0 °C, 1 h, yield: 60–68%, (d) $NaNO_2$, HCl, H_2O, −20 °C, 30 min, then *t*BuSH, 0 °C, 1 h, (e) *t*BuOK, DMSO, rt, over night, yield: 71–77% for 2 steps.

2-alkyl-6-methylaniline (**Y9**), led to corresponding bromoindazoles **Y1c** and **Y1e**. However, since the commercially availability of vinylboronic acids was also poor, alternative methods were desired to prepare A-443654 analogs with more diverse substituents at the C7 position. Thus we investigated a synthetic route as shown in Scheme 5 using direct alkyl-substitution of 2-bromo-6-methylnitorobenzene (**Y12**) by Suzuki coupling under a Hartwig catalyst.[20] Suzuki coupling of **Y12** with alkylboronic acids under the catalysis of $Pd(dba)_2$ and Q-phos, followed by reduction of the nitro group successfully afforded 2-alkyl-6-methylaniline (**Y13**). In this reaction, it was necessary to use 2-bromo-6-methylnitorobenzene (**Y12**) as a starting material instead of 2-bromo-6-methylaniline (**Y8**) because the nitro group activates the arylbromide and under the condition of palladium-Q-phos, the aniline group would likely be reactive. The resulting **Y13** was converted to **Y1** with the same procedure as shown above.

Analogues of A-443654 having a methyl group at the C3 position on the indazole ring were synthesized as depicted in

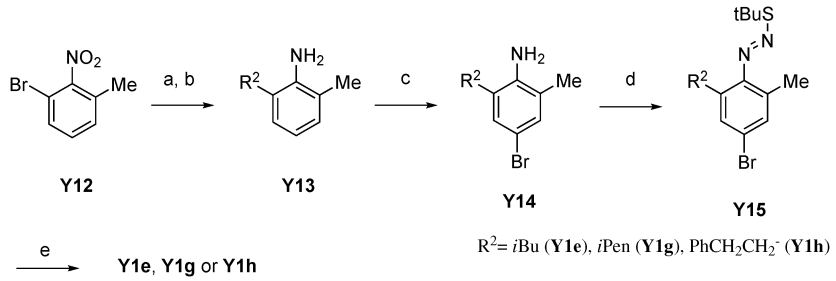

Scheme 5 (a) $R^2B(OH)_2$, $Pd(dba)_2$, K_3PO_4, Q-Phos, toluene, 100 °C, 2.5 h, (b) H_2, Pd/C, EtOH, rt, over night, (c) Br_2, AcOH, 0 °C, 1 h, yield: 24–63% for 3 steps, (d) $NaNO_2$, HCl, H_2O, −20 °C, 30 min, then *t*BuSH, 0 °C, 1 h, (e) *t*BuOK, DMSO, rt, over night, yield: 48–81% for 2 steps.

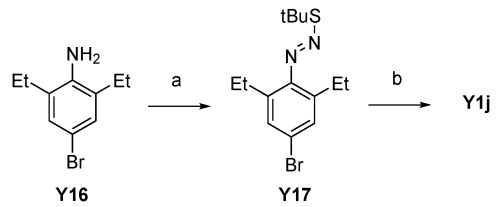

Scheme 6 (a) $NaNO_2$, HCl, H_2O, −20 °C, 30 min, then *t*BuSH, 0 °C, 1 h, (b) *t*BuOK, DMSO, rt, over night, yield: 86% for 2 steps.

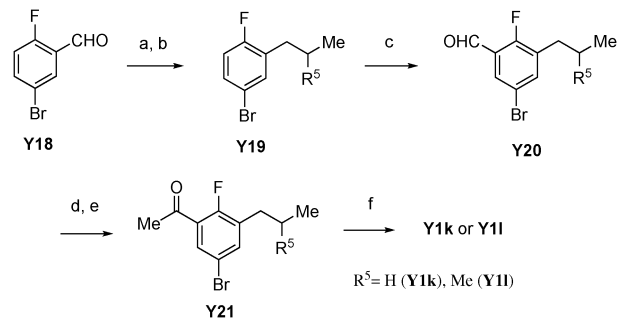

Scheme 7 a) $[Ph_3P\text{-}CHMeR^5]^+Br^-$, *t*BuOK / THF, 2–3 h, (b) H_2, Pd/C, THF, rt, over night (R^5 = H) or $TsNH_2NH_2$, THF, 100 °C, 3 h (R^5 = Me), (c) LDA, THF, −78 °C, 1 h then DMF–THF, −78 °C, 1 h, yield: 47–53% for 3 steps, (d) MeMgBr, Et_2O, 0 °C, 30 min, (e) MnO_2, dioxane, 90 °C, 9 h, yield: 63–88% for 2 steps, (f) NH_2NH_2, DMF, 120 °C, 24 h, yield: 7–11%.

Scheme 6 and Scheme 7. An intermediate with an ethyl substituent at C7 position (**Y1j**) was synthesized with the same procedure as shown above owing to its symmetrical structure (Scheme 6). Due to a lack of ring closure selectivity in an asymmetrical azosulfide, an alternative synthesis for analogues with a larger alkyl group substitution at C7 position was investigated (Scheme 7). Wittig reaction of commercially available aldehyde **Y18** afforded a styrene intermediate which was reduced to linear (**Y19k**, R^5 = H) or branched (**Y19l**, R^5 = Me) alkyl chain with hydrogenation or diimide reduction, respectively.[21] In the hydrogenation to produce **Y19k**, use of THF as a solvent was essential and reaction in either ethyl acetate or ethanol did not give the product. In the case of tri-substituted styrene reduction to give **Y19l**, palladium-carbon hydrogenation in any solvent did not yield the desired product. To avoid the use of a more reactive catalyst for hydrogenation in order not to lose the bromide functional group at 4-position, diimide reduction was tested, affording the saturated alkylbenzene (**Y19l**) without loss of the bromide. Fluorine group-directed ortho lithiation[22] followed by treatment with DMF gave formylbenzene (**Y20**), which was converted to methylketone (**Y21**) by Grignard reaction followed by oxidation of the resulting alcohol. Ring closure using excess amount of hydrazine afforded desired 3-methylindazole (**Y1k** and **Y1l**) but the yield of the reaction was poor because of the sterically hindered nature of the fluorine center.

Analogue sensitive Akt generation and evaluation

To establish the analogue sensitive system for all Akt isoforms, mutations enlarging the size of the ATP-binding pocket were introduced by substituting the gatekeeper methionine (M) with glycine (G) or alanine (A) (*i.e.* M227A/M225A/M229A for Akt1/2/3-*as*1 and M227G/M225G/M229G for Akt1/2/3-*as*2). *In vitro* immunoprecipitation kinase assays revealed that both Ala and Gly mutants of all three isoforms of Akt-*as* retained approximately 30% of the activity of the corresponding Akt-*wt* isoforms (Fig. 2a). The level of Akt1/2/3-*as*1/2 activity in cells was also determined by measurement of GSK-3β Ser-9 phosphorylation. Akt constructs containing a c-Src myristoylation recognition sequence (myr-HA-Akt-*as*) are constitutively membrane localized and thus constitutively active without growth factor stimulation. As expected, expression of myr-HA-Akt1/2/3-*as*1/2 or myr-HA-Akt1/2/3-*wt* in HEK293 cells resulted in elevated phosphorylation of the Akt substrate GSK3β at Ser9 (Fig. 2b). Elevation of GSK3β phosphorylation by myr-HA-Akt1/2/3-*as*1/2 transfection was comparable to that by myr-HA-Akt1/2/3-*wt* transfection, confirming the cellular activity of each Akt-*as* isoform is similar to the corresponding activity of Akt-*wt* isoforms despite the significantly lower measured *in vitro* activity.

Development of Akt-*as* selective inhibitors

With sufficiently active Akt-*as* isoforms in hand, we next sought to develop Akt-*as* specific inhibitors that do not perturb endogenous Akt-*wt* and related kinases. The pyrazolopyrimidine1 (PP1) scaffold has proven to be a versatile starting point for the development of many analog sensitive kinase inhibitors.[15] Over 60% of the analog sensitive kinases we have characterized are potently (<25 nM IC_{50} @ 1 μM ATP) inhibited by one or more of the following pyrazolopyrimidine analogs (1-NM-PP1, 1-NaPP1, or 3-MB-PP1) (C.Z. and K.M.S., unpublished data). In the case of Akt1-*as*2 however, none of these three widely used inhibitors were potent ligands for the engineered kinase although 1-NM-PP1 exhibited the

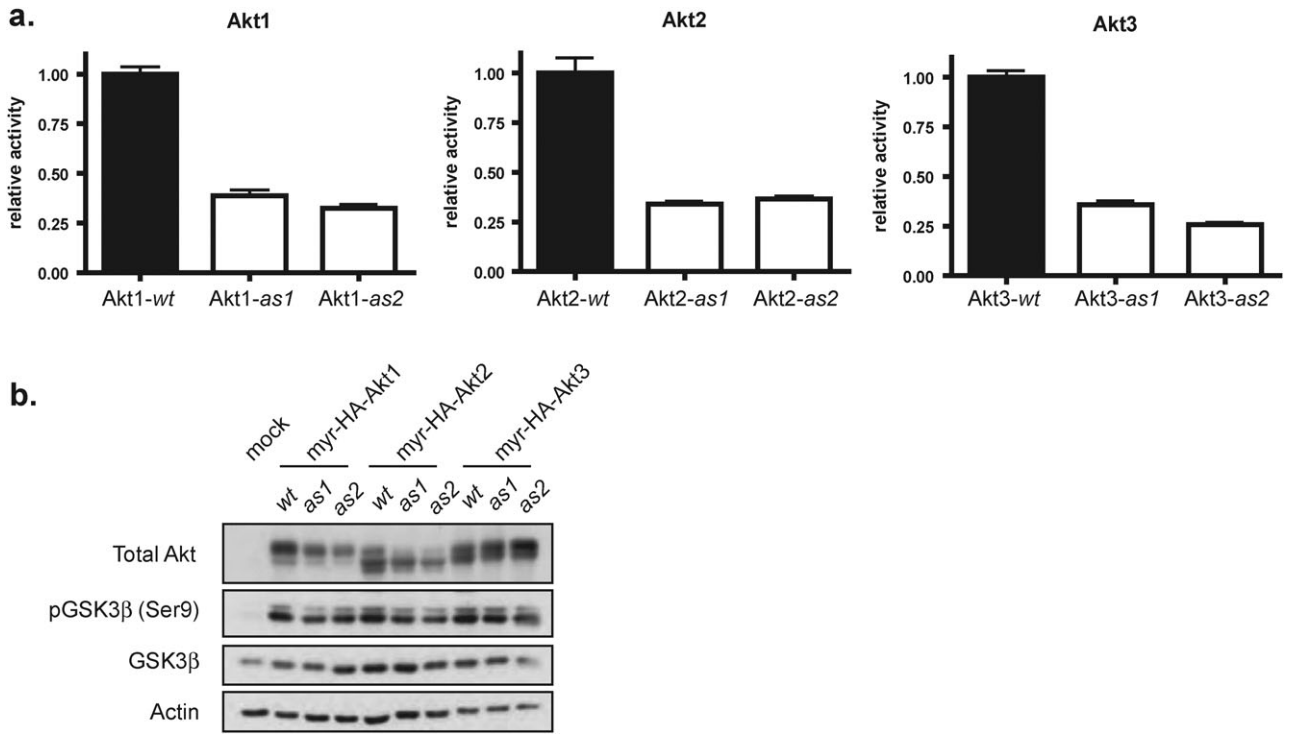

Fig. 2 (a) *In vitro* kinase activity of *wt* and analog sensitive (*as*) Akt kinases. (b) *in vivo* kinase activity of *wt* and *as* kinase activity. Myristoylated Akt was transfected into HEK293T cells and blotted for Akt substrates.

most promising level of inhibition (IC_{50} = 61 nM). A more diverse series of benzyl substituted pyrazolopyrimidine analogues were screened against Akt1/2/3-*as*1/2 at a single concentration (1 uM), leading to the discovery of some modest hits. Most of the hits from the screening have a substituent at the *meta* position on the benzyl group as often seen for SAR against other *as*-kinases. Determination of IC_{50} values of these hits (Table 1) led to the identification of the most potent analogue: 3-iodobenzyl PP1 (**X1b**, **3-IB-PP1**). This molecule inhibits Akt1/2/3-*as*1/2 with good potency, without inhibiting Akt1/2/3-*wt* (Table 1). The *in vitro* potency and selectivity of 3-IB-PP1 for Akt1-*as*1/2 (IC_{50} = 18 nM for *as*1, 28 nM for *as*2) *vs.* Akt1-*wt* (IC_{50} > 10 000 nM) provides a valuable tool for cellular studies of Akt1 specific functions. In contrast, the potency of 3-IB-PP1 for Akt2-*as*1/2 (IC_{50} = 1100 nM for *as*1, 240 nM for *as*2) and Akt3-*as*1/2 (IC_{50} = 76 nM for *as*1, 120 nM for *as*2) is insufficient for an ATP-competitive kinase inhibitor.[23] Although 3IB-PP1 exhibited suitable potency against Akt1-as, the 10-fold drop in potency upon application to Akt2 or Akt3-as alleles precludes their use to study these important Akt isoforms.

To obtain a more effective Akt-*as*1/2 specific inhibitor, we turned to a scaffold based on the known pan-Akt inhibitor A-443654. The parent compound exhibits unusual potency against Akt (Ki = 160 pM for Akt1) and a co-crystal structure was available to guide derivative design. Evaluation of the crystal structure[24] of Akt2 with A-443654 suggested the C7 position on the indazole ring of A-443654 to be a promising position for introducing large substituents that would clash with the gatekeeper methionine of Akt-*wt* (Fig. 1b). SAR studies of various C7 substituted A-443654 analogues were carried out. Since the distance between the methylthio group of the gatekeeper methionine and C7-carbon on A-443654 is 3.7 Å (resolution: 2.30 Å), a small alkyl group was substituted for hydrogen on the C7 position on the indazole ring. We hypothesized a neutral group such as a hydrocarbon chain was a suitable substitution in order not to disrupt already existing H-bonds. Substitution at the C6 position was also considered but we were concerned about changing the dihedral angle between the indazole ring and the pyridine ring.

We first synthesized analogues without a methyl group at the C3 position of the indazole moiety because of synthetic accessibility of this series (R^2 = H). A-443654 analogues having a methyl group at C3 position are previously reported to be ~5-fold more potent against Akt than the corresponding 3-hydrogen-derivartives.[18] We thus planned to introduce a 3-methyl substituent on 3-hydrogen-analogues having an optimized C7 substituent. As shown in Table 2, introduction of a methyl group (**Y4a**) to the C7 position does not inhibit Akt-*wt*, suggesting a small substituent such as a methyl group is sufficient to exhibit orthogonality against Akt-*wt* presumably by clashing with the gatekeeper methionine. Moreover **Y4a** weakly inhibited Akt-*as* isoforms.

Encouraged by these results, we next synthesized 3-hydrogen analogues with a larger alkyl substituent at C7 position on the indazole ring (**Y4b–Y4i**). Assays against Akt-*as* isoforms revealed that these analogues potently inhibit Akt-*as*2. Interestingly the derivatives do not show strong inhibition against Akt-*as*1 isoform. It remains unclear why this reduced potency exists for the Akt-*as*1 isoform. However, the methyl side chain of the mutated alanine residue at gatekeeper position (*as*1) may clash with the substituent at the C7 position

Table 1 IC_{50} values of pyrazolopyrimidine series **X1** against *wt* and *as* Akt1/2/3

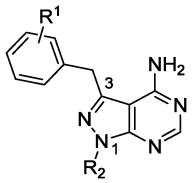

X1

Compd	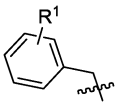	R^2	Akt variants IC_{50} (nM)								
			Akt1-*as*1	Akt1-*as*2	*wt*Akt1	Akt2-*as*1	Akt2-*as*2	*wt*Akt2	Akt3-*as*1	Akt3-*as*2	*wt*Akt3
X1a	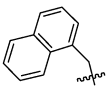	*t*Bu	71	61	> 10 000	1200	280	> 10 000	150	110	> 10 000
X1b(3-IB-PP1)	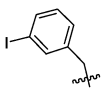	*t*Bu	18	28	> 10 000	1100	240	> 10 000	76	120	> 10 000
X1c	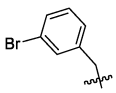	*t*Bu	32	60	> 10 000	520	380	> 10 000	78	90	> 10 000
X1d	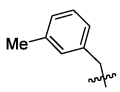	*t*Bu	67	84	> 10 000	N.D.	360	> 10 000	63	150	> 10 000
X1e	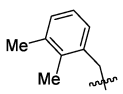	*t*Bu	71	100	> 10 000	1000	320	> 10 000	72	84	> 10 000
X1f	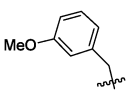	*t*Bu	61	180	> 10 000	1100	860	> 10 000	130	340	> 10 000
X1g		*t*Bu	290	660	> 10 000	1900	4900	> 10 000	260	800	> 10 000
X1h	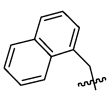	*t*Pr	120	140	> 10 000	N.D.	1200	> 10 000	250	110	> 10 000
X1i	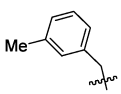	Cyclo Pen	81	110	> 10 000	N.D.	470	> 10 000	82	150	> 10 000

on the inhibitors. Compounds having relatively larger alkyl groups at C7 position potently inhibit Akt-*as*2 and surprisingly, even compounds with a very large substituent such as phenethyl (**Y4h**) potently inhibit Akt-*as*2, suggesting existence of a large pocket behind the gatekeeper. Maximum potency occurred with C_3–C_5 alkyl substituents at C7 (**Y4c–Y4g**). As anticipated based on the close proximity of these substituents to the gatekeeper sidechain, these analogues did not inhibit Akt-*wt*.

Finally we attempted to gain additional potency by exploiting the known enhancement of Akt potency by derivatization at the C3 position. Due to the preference for rigid substituents, we chose **X4b** (Et), **X4c** (nPr) and **X4e** (iBu) for further derivatization at C3 position. As anticipated based on SAR studies by the Abbott group, introduction of a C3-methyl substituent dramatically improved (*ca.* 10-fold) the binding affinity to afford compounds showing excellent potency against all isoforms of Akt-*as*2 (low-nanomolar-range IC_{50} against all isoforms of Akt-*as*2) (**Y4k** and **Y4l**). We chose **Y4k** as the optimal inhibitor for each analog specific Akt isoform and named it **PrIDZ** (Propylindazole).

Specificity and cellular effects of Akt-*as* selective inhibitors

With inhibitors **PrIDZ** and **3-IB-PP1** optimized against Akt1/2/3-*as*, we sought to confirm their orthogonality against the human kinome both *in vivo* and *in vitro*. To assess their specificity for Akt-*as*, we screened both compounds against

Table 2 IC_{50} values of indazole series **Y4** against *wt* and *as* Akt1/2/3

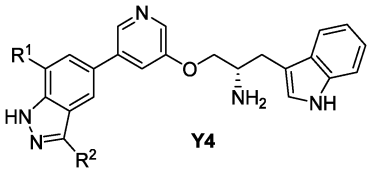

				Akt variants IC_{50} (nM)								
Compd	Scheme	R^1	R^2	Akt1-*as*1	Akt1-*as*2	*wt*Akt1	Akt2-*as*1	Akt2-*as*2	*wt*Akt2	Akt3-*as*1	Akt3-*as*2	*wt*Akt3
Z(A-443654)	1	H–	Me–	ND	ND	3	ND	ND	30	30	ND	51
Y4a	2	Me–	H–	240	100	>1000	>1000	>1000	>1000	>1000	>1000	>1000
Y4b	2	Et–	H–	860	25	570	>1000	930	>1000	>1000	770	>1000
Y4c	4	*n*Pr–	H–	330	6	>1000	>1000	110	>1000	>1000	63	>1000
Y4d	3	*n*Bu–	H–	350	4	>1000	>1000	43	>1000	530	33	>1000
Y4e	5	*i*Bu–	H–	>1000	6	>1000	>1000	19	>1000	>1000	28	>1000
Y4f	4	*n*Pen–	H–	380	26	>1000	>1000	58	>1000	750	34	>1000
Y4g	5	*i*Pen–	H–	270	17	>1000	>1000	35	>1000	300	25	>1000
Y4h	5	$PhCH_2CH_2$–	H–	560	34	>1000	>1000	100	>1000	630	50	>1000
Y4i	2	Cl–	H–	320	87	720	>1000	700	>1000	>1000	>1000	>1000
Y4j	6	Et–	Me–	270	17	740	>1000	200	>1000	900	110	>1000
Y4k (PrIDZ)	7	*n*Pr–	Me–	56	2.8	>1000	>1000	31	>1000	360	13	>10000
Y4l	7	*i*Bu–	Me–	720	6.6	>1000	>1000	6.7	>1000	>1000	25	>10000

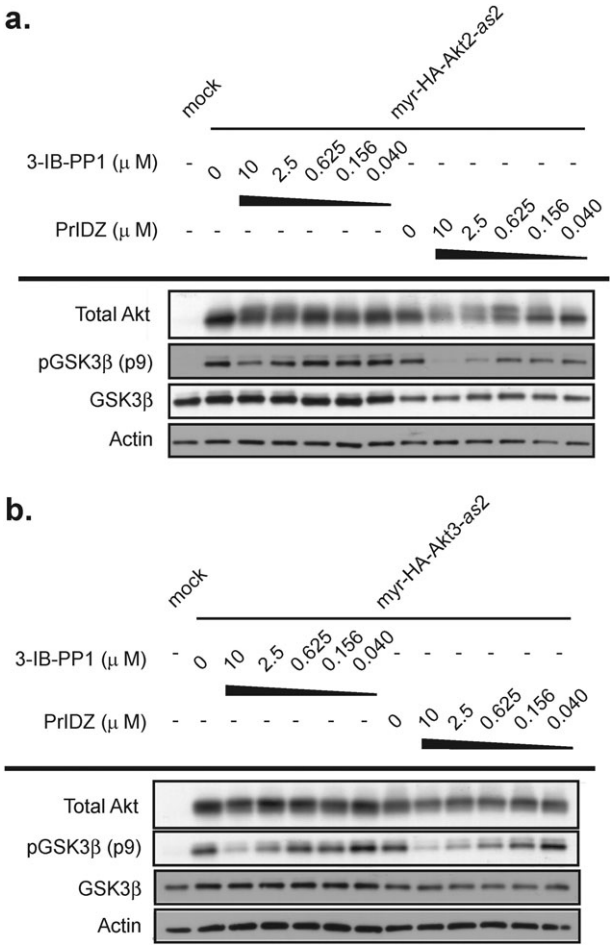

Fig. 3 *In vivo* activity of engineered inhibitors 3-IB-PP1 and PrIDZ in HEK 293 cells transfected with myristoylated analog sensitive Akt2 (a) or Akt3 (b).

191 human kinases and disease mutants using the SelectScreen® kinase profiling service from Invitrogen (Supplementary Table 1). Compared to the parent compound, A-443654, which we previously reported inhibited 47/220 kinases at 1 μM,[13] the **PrIDZ** analog was far more selective. Only 10 kinases were inhibited at greater than 80% at 5 μM and none were found in the canonical PI3K → Akt → mTOR signaling pathway. **3-IB-PP1** was similarly selective, only inhibiting 9 kinases at 5 μM and only one of these kinases was also inhibited by **PrIDZ** (Casein Kinase 1δ, CK1δ). Together these results validate our analog sensitive strategy and confirm that any results observed with the two inhibitors are likely due to on-target effects against Akt-*as*.

We next validated the ability of compounds **PrIDZ** and **3-IB-PP1** to effectively and potently inhibit Akt-*as*2 kinases expressed in cells. We previously validated the cellular orthogonality of our inhibitors against Akt-*wt*, by measuring *in vivo* inhibition of downstream Akt targets by our engineered compounds and the parent A-443654 and observed no cross-reactivity.[13] The data confirm that these *as*-specific inhibitors are sufficiently selective against Akt-*wt*, and that as predicted from the *in vitro* screening, off-target effects of these compounds do not have observable effects on upstream or downstream of Akt.

Cellular effects of these inhibitors (**PrIDZ** and **3-IB-PP1**) against Akt-*as*2 isoforms were assessed in HEK 293 cells transfected with the constitutively activated myr-HA-Akt1/2/3-*as*2. Treatment of cells transfected with myr-HA-Akt1/2/3-*as*2 with various concentrations of **PrIDZ** and **3-IB-PP1** was performed to analyze the phosphorylation status of GSK3β (Fig. 3) (Akt1 previously reported in ref. 13). Both inhibitors decreased the phosphorylation level of Ser9 on GSK3β in a dose-dependent manner and **PrIDZ** was particularly effective at inhibiting Akt-*as*2, validating *in vitro* inhibitory activities

(IC_{50} values could not be independently determined from western blots). The data suggested that the treatment of cells expressing Akt-*as*2 isoforms with **PrIDZ** is an effective means of potently inhibiting each of the three Akt isoform functions in cells.

Conclusion

In an effort to develop highly specific inhibitors of each individual human kinase we have developed a widely used chemical genetic method that exploits the conserved nature of the gatekeeper residue across the kinome. This method has been applied widely using a pyrazolopyrimidine based scaffold for inhibition of kinases engineered to contain a Gly or Ala gatekeeper residue. It is perhaps not surprising that a single scaffold would be unable to potently bind all engineered kinases, since the PP1 scaffold was first identified by Pfizer as an inhibitor of the Src tyrosine kinase family.[15] In attempting to develop a potent inhibitor of the serine threonine kinase Akt, we found that the pyrazolopyrimidine scaffold could be tuned to inhibit analog sensitive Akt1, but we were unable to potently inhibit the Akt2 or Akt3 isoforms with this inhibitor class. In order to achieve more potent inhibition of all Akt isoforms we turned to the Akt inhibitor A-443654 from Abbott based on the indazole scaffold. Modifications at the C-7 position rendered the inhibitor unable to bind to *wt* Akt isoforms yet while retaining the ability to potently inhibit each of the three Akt-*as* isoforms.

These studies provide an additional avenue to development of chemical genetic inhibitors of a wide variety of kinases. The extensive expansion of drug discovery efforts focused on protein kinases have afforded many new scaffolds that as our work shows can be relatively easily repurposed for the development of mutant specific kinase inhibitors. In addition to the development of potent inhibitors, there is an additional benefit to extension beyond the pyrazolopyrimidine scaffold. As with any small molecule used in complex biological systems, one must always be concerned with off-target effects due to binding of the particular molecule to unintended targets. This concern is greatly ameliorated by the use of a chemical genetic system, which allows side-by-side comparison of cells containing a single point mutation in a single target within an isogenic cell line. Nonetheless, another type of control based on changing the inhibitor structure is beneficial. The use of a second chemical series with comparable *in vitro* specificity for the target of interest (Akt-*as*) can be used in cellular experiments. If the cellular effects of the two structurally distinct compounds are similar, then one can gain increasing confidence in effects being on-target. The key assumption is that compounds with vastly different structure may share one target in common but are largely unlikely to share a common off target effect.

The development of this chemical genetics approach complements traditional genetic techniques.[25,26] An analog sensitive kinase and inhibitor can phenocopy the selectivity of genetic knockouts while being reversible and temporally controllable. Heat sensitive or drug inducible knockout systems do allow for control of gene expression but both are binary in nature and neither offer the simple and rapid titration of kinase activity possible with chemical genetics. Generation of analog sensitive model organisms can allow for the deconvolution of kinase function required in development versus adult homeostasis.[16] Many of the isoform specific effects in Akt knockout mice were gross developmental defects that might differ significantly from knocking out the kinase in adults. Generation of Akt-*as* mice would allow for the elucidation of the role of Akt isoforms in adult biology and may more directly inform upon their contributions to cancer where Akt dysregulation is clinically implicated.

The availability of potent and specific Akt inhibitors that bind in the ATP site allowed recent elucidation of a new form of kinase inhibition. Kinase dead Akt mutants treated with selective inhibitors became hyperphosphorylated independent of downstream kinase activity.[13] This demonstrated a new mode of kinase activation whereby conformational changes induced by inhibitor binding altered the kinase's accessibility to being phosphorylated by upstream kinases. This observation illustrates the complexity inherent in signaling networks and the frequent unexpected feedback loops present in these systems.

Experimental

Buffer solutions

Buffer A: 20 mM Tris (pH 7.5), 150 mM NaCl, 1 mM EDTA, 1 mM EGTA, 1% (v/v) Triton X, 2.5 mM sodium pyrophosphate, 1 mM β-glycerphosphate, Complete protease inhibitor cocktail (Roche Applied Sciences), phosphatase inhibitor cocktail 1 (Sigma-Aldrich), phosphatase inhibitor cocktail 2 (Sigma-Aldrich), and 20 nM microcystin LR (Calbiochem). Buffer B: 25 mM Tris (pH 7.5), 10 mM $MgCl_2$, 5 mM β-glycerphosphate, 0.1 mM sodium orthovanadate and 2 mM DTT.

In vitro kinase assays

HEK293T cells were plated in six-well dishes and transfected at approximately 90% confluence with the appropriate pcDNA3-myr-HA-Akt1/2/3-*as*1/2 plasmid using Lipofectamine 2000 (Invitrogen) in accordance with the manufacturer's instructions. After 48 h cells were washed and detached with Ca^{2+}, Mg^{2+} free ice cold PBS and pelleted by centrifugation at 14 000*g* for 20 min at 4 °C. Pellets were lysed using Buffer A then immunoprecipated overnight at 4 °C by using anti-HA Affinity Matrix (Roche Applied Science) pre-blocked with 1% BSA in PBS. Immunoprecipitates were washed twice with Buffer A and then twice with Buffer B before performing the *in vitro* kinase assay. Serial dilutions of individual inhibitors were incubated with immunoprecipitated myr-HA-Akt constructs, 30 μM synthetic peptide GRPRTSSFAEG (Crosstide, Upstate), 1.7% DMSO, 28 nM (2.5 μCi) [γ-^{32}P]ATP (3000 Ci/mmol, Perkin Elmer Life Science) and 50 μM ATP n Buffer B for 45 min. Reaction mixtures were spotted into phosphocellulose paper (Whatman) and washed 5× with 1% H_3PO_4. Membranes were exposed to a phosphoimager and scanned on Typhoon analyzer (Amersham Biosciences) to quantify the radioactivity with SPOT software.[27]

Immunoblots

After appropriate stimulation and/ or drug treatment HEK 293 cells were pelleted and lysed as described for the *in vitro* kinase assays. Cell lysates were subjected to SDS/PAGE and transferred to nitrocellulose membranes (Bio-Rad Laboratories). Blots were blocked with 5% (w/v) skim milk in 0.1% (v/v) Tween-20/Tris-buffered Saline (TBST). They were then probed with various primary antibodies in 5% BSA (w/v) in TBST according to manufacture's instructions (All primary antibodies from Cell Signaling Technology). Primary antibodies were detected by appropriate peroxidase-conjugated IgGs (Pierce Biotechnology or Santa Cruz Biotechnology) in 5% (w/v) BSA/TBST and protein signal was visualized using enhanced chemoluminescence (Pierce Biotechnology) by exposure to CL-X Posure film (Pierce Biotechnology).

Plasmid constructs

pcDNA3-myr-HA-Akt1/2/3 were kind gifts of W. Sellers *via* Addgene (Akt1/2/3)-Addgene plasmid 9008/9016/9017). Point mutations in Akt for the gatekeeper were introduced by a modified method of Stratgene QuikChange® site-directed mutagenesis (SQC).[28] Generation of Akt1/2/3-*as*2 (M → G gatekeeper mutation) was described previously in the supplemental methods to ref. 13. Akt1/2/3-*as*1 (M227A, M229A and M225A respectively) were generated using the same methods with the following Quikchange primers. M227A in Akt1 (fwd: 5′ TT GTC gcc GAG TAC GCC AAC GGG GGC GAG CTG TTC, rev: 5′ TA CTC ggc GAC AAA GCA GAG GCG GTC GTG GGT CTG); M229A in Akt2 (fwd: 5′ TT GTG gcc GAG TAT GCC AAC GGG GGT GAG CTG TTC, rev: 5′ TA CTC ggc CAC AAA GCA CAG GCG GTC GTG GGT CTG); M225A in Akt3 (fwd, 5′ GT TTT GTG gcc GAA TAT GTT AAT GGG GGC GAG CTG, rev 5′ C ATA TTC ggc CAC AAA ACA CAA ACG GTC TTT TGT C).

Accession code

Protein Data Bank: The cocrystal structure of Akt2 with A-443654 was generated in a previous study and deposited under accession code 2JDR.

Chemical synthesis

Unless otherwise noted, all reactions were performed under argon and stirred magnetically in oven-dried glassware fitted with rubber septa. All ^{1}H and ^{13}C NMR were recorded on a Varian Innova 400 spectrometer at 400 MHz and 100 MHz, respectively. ^{1}H chemical shifts are reported as chemical shifts (δ) in ppm, multiplicity (s: singlet; d: doublet; t: triplet; dd: doublet of doublets; m: multiplet; br: broad), number of protons and coupling constant (*J*) in hertz (Hz). ^{13}C NMR data are reported as chemical shifts (δ) in ppm and coupling constant (*J*) in hertz (Hz) for C-F coupling. Low resolution electrospray ionization LCMS (LR ESI-LCMS) and liquid chromatography retention times were recorded on a Waters Micromass ZQ equipped with a Waters 2695 Separations Module using an XTerra MS C18 3.5 μm column (Waters). Retention times were obtained using an initial flow rate of 1 mL/min of 95% A (H_2O with 0.1% formic acid) and 5% B (CH_3CN with 0.1% formic acid) for 0.5 min followed by a linear gradient with a flow rate of 0.5 mL/min of 95% A and 5% B to 5% A and B in 4.5 min followed by 0.5 min at of 5% A and 95% B. High-resolution electron impact mass spectra were recorded on a MicoMass VG70E spectrometer at the University of California-San Francisco center for Mass Spectrometry. Preparative HPLC was performed on a Varian ProStar solvent delivery system equipped with a Zorbax 300-SB C18 column using a CH_3CN (0.1% TFA)/H_2O (0.1% TFA) gradient (0–100%) as the mobile phase and monitored by UV at $\lambda = 254$ nm. Automated silica gel chromatography was performed on an AnaLogix IntelliFlash 280 system using Analogix SuperFlash Sepra Si 50 columns and monitored by UV at $\lambda = 254$ nm. Unless otherwise noted, all reagents and solvents were obtained from commercial suppliers and were used without further purification.

A-443654 derived analogs

5-bromo-7-methyl-1*H*-indazole (Y1a). To a suspension of aniline **Y6a** (2.0 g, 10.0 mmol) in 24% hydrochloric acid (5.5 ml) was added a solution of sodium nitrite (730 mg, 10.5 mmol) in water (1.6 ml) dropwise at −20 °C. After stirring for 30 min at −20 °C, the mixture was buffered to *ca.* pH 5 with solid sodium acetate. The mixture was added to a solution of *tert*-butylthiol (1.10 ml, 10.0 mmol) in ethanol at 0 °C and stirred at rt for 1 h. After dilution with ethyl acetate, the organic layer was and then dried and concentrated to give diazosulfide **Y7a** (3.6 g). A solution of **Y7a** (3.6 g) in DMSO was added potassium *tert*-butoxide (9.9 g, 88.2 mmol) at 0 °C and the mixture was stirred over night at rt. The reaction was quenched with 1 M HCl aq. at 0 °C and diluted with ethyl acetate. The organic layer was washed with water and then dried and concentrated. The resulting residue was purified by column chromatography on silica gel (hexane-ethyl acetate gradient) to afford **Y1a** (1.5 g, 7.11 mmol, 71% for 2 steps). ^{1}H NMR (400 MHz, $CDCl_3$) δ 2.60 (s, 3H), 7.34 (s, 1H), 7.78 (s, 1), 8.09 (s, 1H). LR ESI-LCMS *m*/*z* calculated 211, 213, found 211, 213 $[M+H]^+$.

5-bromo-7-ethyl-1*H*-indazole (Y1b). To a suspension of aniline **Y5b** (2.0 g, 14.8 mmol) in acetic acid (8.0 ml) was added a solution of Br_2 (800 μl, 15.5 mmol) in acetic acid (8 ml) dropwise at 0 °C. After stirring for 2.5 h at 0 °C, the mixture was diluted with ethyl acetate and water, and then neutralized with 6 M NaOHaq. The organic layer was washed with sat. $Na_2S_2O_3$aq. and then dried and concentrated. The resulting residue was purified by column chromatography on silica gel (hexane-ethyl acetate gradient) to afford **Y6b** (2.8 g, 13.1 mmol, 88%) of sufficient purity to carry on to the next step. Compound **Y1b** was synthesized from **Y6b** (2.8 g, 13.1 mmol) according to the procedure for **Y1a** by substituting **Y6b** for **Y6a**. Yield: 1.9 g (8.4 mmol, 64% for 2 steps). ^{1}H NMR (400 MHz, $CDCl_3$) δ 1.34 (t, $J = 5.8$ Hz, 3H), 2.88 (t, $J = 7.6$ Hz, 2H), 7.26 (s, 1H), 7.71 (s, 1H), 7.99 (s, 1H). LR ESI-LCMS *m*/*z* calculated 225, 227, found 225, 227 $[M+H]^+$.

5-bromo-7-chloro-1*H*-indazole (Y1i). Compound **Y1i** was synthesized from **Y6i** (3.2 g, 14.4 mmol) according to the procedure for **Y1a** by substituting **Y6i** for **Y6a**. Yield: 1.8 g (7.8 mmol, 54% for 2 steps). ^{1}H NMR (400 MHz, DMSO-d_6)

δ 7.65 (s, 1H), 8.02 (s, 1H), 8.19 (s, 1H). LR ESI-LCMS *m*/*z* calculated 231, 233, found 231, 233 $[M+H]^+$.

4-bromo-2-methyl-6-propylbenzenamine (Y10c). To a solution of bromobenzene **Y8** (3.5 g, 18.8 mmol) in DME (94 ml) and water (23 ml) were added $Pd(PPh_3)_4$ (1.2 g, 1.0 mmol), Na_2CO_3 (2.0 g, 18.8 mmol) and *trans*-1-propen-1-ylboronic acid (2.03 g, 23.6 mmol). After stirring over night at 85 °C, the mixture was diluted with ethyl acetate. The organic layer was washed with water and then dried and concentrated. The resulting residue was purified by column chromatography on silica gel (hexane-ethyl acetate gradient) to afford the styrene analogue (2.5 g) of sufficient purity to carry on to the next step. To a solution of the styrene analogue (2.5 g) in ethanol (40 ml) was added 20% Pd-C wet (500 mg) and the mixture was stirred over night at rt under H_2 atmosphere. After filtration over Celite, the solvent was removed *in vacuo* to give crude **Y9c** (2.1 g, 14.3 mmol, 76% for 2 steps). The crude product **Y9c** was used for the next step without further purification. To a solution of **Y9c** (2.6 g, 17.4 mmol) in acetic acid (13 ml) was added a solution of Br_2 (940 µl, 18.3 mmol) in acetic acid (13 ml) dropwise at 0 °C. After stirring for 1 h at 0 °C, the mixture was diluted with ethyl acetate and water, and then neutralized with 6 M NaOH aq. The organic layer was washed with sat. $Na_2S_2O_3$ aq. and then dried and concentrated. The resulting residue was purified by column chromatography on silica gel (hexane-ethyl acetate gradient) to afford **Y10c** (2.7 g, 11.9 mmol, 68%). ^{1}H NMR (400 MHz, $CDCl_3$) δ 0.98 (t, *J* = 7.4 Hz, 3H), 1.59–1.65 (m, 2H), 2.16 (s, 3H), 2.44 (t, *J* = 7.6 Hz, 2H), 7.04 (d, *J* = 4.4 Hz, 2H). LR ESI-LCMS *m*/*z* calculated 228, 230, found 228, 230 $[M+H]^+$.

5-bromo-7-propyl-1*H*-indazole (Y1c). Compound **Y1c** was synthesized from **Y10c** (2.7 g, 11.8 mmol) according to the procedure for **Y1a** by substituting **Y10c** for **Y6a**. Yield: 2.0 g (8.37 mmol, 71% for 2 steps). ^{1}H NMR (400 MHz, $CDCl_3$) δ 1.04 (t, *J* = 7.4 Hz, 3H), 1.77-1.85 (m, 2H), 2.91 (t, *J* = 7.6 Hz, 2H), 7.35 (s, 1H), 7.79 (s, 1H), 8.10 (s, 1H). LR ESI-LCMS *m*/*z* calculated 239, 241, found 239, 241 $[M+H]^+$.

4-bromo-2-methyl-6-pentylbenzenamine (Y10f). Compound **Y10f** was synthesized from **Y8** (5.5 g, 28.1 mmol) according to the procedure for **Y10c** by substituting 1-penten-1-ylboronic acid for *trans*-1-propen-1-ylboronic acid. Yield: 2.7 g (10.4 mmol, 37% for 3 steps). ^{1}H NMR (400MHz, $CDCl_3$) δ 0.91 (d, *J* = 6.4 Hz, 3H), 1.36 (m, 4H), 1.60 (m, 2H), 2.15 (s, 3H), 2.44 (t, *J* = 7.8 Hz, 2H), 7.05 (s, 2H). LR ESI-LCMS *m*/*z* calculated 256, 258, found 256, 258 $[M+H]^+$.

5-bromo-7-pentyl-1*H*-indazole (Y1f). Compound **Y1f** was synthesized from **Y10f** (500 mg, 1.95 mmol) according to the procedure for **Y1a** by substituting **Y10f** for **Y6a**. Yield: 400 mg (1.50 mmol, 77% for 2 steps). ^{1}H NMR (400 MHz, $CDCl_3$) δ 0.91 (t, *J* = 7.0 Hz, 3H), 1.39 (m, 4H), 1.76 (m, 2H), 2.85 (t, *J* = 7.8 Hz, 2H), 7.28 (s, 1H), 7.75 (s, 1H), 8.01 (s, 1H). LR ESI-LCMS *m*/*z* calculated 267, 269, found 267, 269 $[M+H]^+$.

4-bromo-2-*iso*butyl-6-methylbenzenamine (Y14e). To a solution of nitrobromobenzene **Y12** (4.0 g, 18.5 mmol) in toluene (80 ml) were added bis(dibenzylideneacetone)palladium(0) (106 mg, 0.185 mmol), 1,2,3,4,5-pentaphenyl-1′-(di-*tert*-butylphosphino)ferrocene (285 mg, 0.37 mmol), K_3PO_4 (7.8 g, 37.0 mmol) and *iso*butylboronic acid (2.26 g, 22.2 mmol). After stirring for 2.5 h at 100 °C, the mixture was diluted with ethyl acetate. The organic layer was washed with 1 M HCl aq. and 1 M NaOH aq., and then dried and concentrated. The resulting residue was purified by column chromatography on silica gel (hexane-ethyl acetate gradient) to afford the dialkylnitrobenzene analogue (3.5 g) of sufficient purity to carry on to the next step. To a solution of the dialkylnitrobenzene analogue (3.5 g) in ethanol (40 ml) was added 20% Pd-C wet (600 mg) and the mixture was stirred over night at rt under H_2 atmosphere. After filtration over Celite, the solvent was removed *in vacuo* to give crude **Y13e** (2.1 g). The crude product **Y13e** was used for the next step without further purification. To a solution of **Y13e** (2.1 g, 14.1 mmol) in acetic acid (8 ml) was added a solution of Br_2 (800 µl, 15.5 mmol) in acetic acid (8 ml) dropwise at 0 °C. After stirring for 1 h at 0 °C, the mixture was diluted with ethyl acetate and water, and then neutralized with 6 M NaOH aq. The organic layer was washed with sat. $Na_2S_2O_3$ aq. and then dried and concentrated. The resulting residue was purified by column chromatography on silica gel (hexane-ethyl acetate gradient) to afford **Y14e** (1.06 g, 4.38 mmol, 24% for 3 steps). ^{1}H NMR (400 MHz, $CDCl_3$) δ 0.95 (d, *J* = 6.4 Hz, 6H), 1.92 (m, 1H), 2.14 (s, 3H), 2.34 (d, *J* = 7.2 Hz, 2H), 7.00 (s, 1H), 7.06 (s, 1H). LR ESI-LCMS *m*/*z* calculated 242, 244, found 242, 244 $[M+H]^+$.

5-bromo-7-*iso*butyl-1*H*-indazole (Y1e). Compound **Y1e** was synthesized from **Y14e** (1.06 g, 4.38 mmol) according to the procedure for **Y1a** by substituting **Y14e** for **Y6a**. Yield: 900 mg (3.56 mmol, 81% for 2 steps). ^{1}H NMR (400 MHz, $CDCl_3$) δ 0.98 (d, *J* = 6.8 Hz, 6H), 2.06 (m, 1H), 2.72 (d, *J* = 7.6 Hz, 2H), 7.25 (s, 1H), 7.76 (s, 1H), 8.01 (s, 1H). LR ESI-LCMS *m*/*z* calculated 253, 255, found 253, 255 $[M+H]^+$.

4-bromo-2-*iso*pentyl-6-methylbenzenamine (Y14g). Compound **Y14g** was synthesized from **Y12** (4.0 g, 18.5 mmol) according to the procedure for **Y14e** by substituting *iso*pentylboronic acid for *iso*butylboronic acid. Yield: 3.0 g (11.7 mmol, 63% for 3 steps). ^{1}H NMR (400 MHz, $CDCl_3$) δ 0.90 (d, *J* = 6.4 Hz, 6H), 1.50 (m, 2H), 1.65 (m, 1H), 2.52 (s, 3H), 2.81 (t, *J* = 8.2 Hz, 2H), 7.20 (s, 2H). LR ESI-LCMS *m*/*z* calculated 256, 258, found 256, 258 $[M+H]^+$.

5-bromo-7-*iso*pentyl-1*H*-indazole (Y14g). Compound **Y1g** was synthesized from **Y14g** (3.0 g, 11.7 mmol) according to the procedure for **Y1a** by substituting **Y14g** for **Y6a**. Yield: 2.0 g (7.49 mmol, 64% for 2 steps). ^{1}H NMR (400 MHz, $CDCl_3$) δ 1.01 (d, *J* = 6.4 Hz, 6H), 1.71 (m, 3H), 3.02 (m, 2H), 7.42 (s, 1H), 7.82 (s, 1H), 8.19 (s, 1H). LR ESI-LCMS *m*/*z* calculated 267, 269, found 267, 269 $[M+H]^+$.

4-bromo-2-methyl-6-phenethylbenzenamine (Y14h). Compound **Y14h** was synthesized from **Y12** (4.0 g, 18.5 mmol) according to the procedure for **Y14h** by substituting phenethylboronic acid for *iso*butylboronic acid. Yield: 2.0 g (6.90 mmol, 37% for 3 steps). ^{1}H NMR (400 MHz, $CDCl_3$) δ 2.15 (s, 3H), 2.73–2.77 (m, 2H), 2.89–2.94 (m, 2H), 7.08 (s, 2H), 7.19–7.33 (m, 5H).

5-bromo-7-phenethyl-1*H*-indazole (Y1h). Compound **Y1h** was synthesized from **Y14h** (2.0 g, 6.90 mmol) according to the procedure for **Y1a** by substituting **Y14h** for **Y6a**. Yield: 1.0 g (3.32 mmol, 48% for 2 steps). ^{1}H NMR (400 MHz, $CDCl_3$) δ 3.03–3.07 (m, 2H), 3.14–3.18 (m, 2H), 7.14–7.15 (m, 2H), 7.24–7.29 (m, 4H), 7.75 (s, 1H), 7.95 (s, 1H). LR ESI-LCMS *m*/*z* calculated 301, 303, found 301, 303 $[M+H]^+$.

5-bromo-7-ethyl-3-methyl-1*H*-indazole (Y1j). Compound **Y1j** was synthesized **Y16** (2.0 g, 8.77 mmol) according to the procedure for **Y1a** by substituting **Y16** for **Y6a**. Yield: 1.8 g (7.53 mmol, 86% for 2 steps). ^{1}H NMR (400 MHz, $CDCl_3$) δ 1.35 (t, J = 7.4 Hz, 3H), 2.54 (s, 3H), 2.86 (q, J = 7.6 Hz, 2H), 7.26 (s, 1H), 7.65 (s, 1). LR ESI-LCMS *m*/*z* calculated 239, 241, found 239, 241 $[M+H]^+$.

5-bromo-2-fluoro-3-propylbenzaldehyde (Y20k). To a solution of ethyltriphenylphosphonium bromide (16.6 g, 44.8 mmol) in THF (230 ml) was added potassium *tert*-butoxide (5.0 g, 44.8 mmol) at 0 °C. After stirring for 10 min at rt, **Y18** (7.0 g, 34.4 mmol) was added, then the mixture was stirred at rt for 3 h. After removal of the solvent in vacuo, the residue was dissolved in EtOAc and filterated through celite. After concentration of the filtrate, the residue was purified by filtration through a pad of silica gel in a large sintered glass funnel eluting with hexanes to afford styrene analogue (12.5 g). To a solution of the styrene analogue (8.4 g) in THF (84 ml) was added 20% Pd–C (wet) (1.7 g), and the resulting mixture was stirred at rt under H_2 atmosphere for 20 h. After filteration on celite, the solvent was removed *in vacuo* to give crude **Y19k** (7.0 g). To a solution of **Y19k** (7.0 g) in dry THF was added 2M solution of LDA in heptanes, THF and ethylbenzene (16.1 ml, 32.2 mmol) at −78 °C and stirred for 1 h at the same temperature. DMF (3.3 ml, 41.9 mmol) was added and the mixture was stirred for additional 1 h at −78 °C. The reaction was quenched with ice chips and diluted with EtOAc. The organic layer was washed with 1N HClaq. and water, and then dried and concentrated. The resulting residue was purified by column chromatography on silica gel (hexane-EtOAc gradient) to afford **Y20k** (4.2 g, 17.1 mmol, 57% for 3 steps). ^{1}H NMR (400 MHz, $CDCl_3$) δ 0.98 (t, J = 7.4 Hz, 3H), 1.68 (m, 2H), 2.66 (t, J = 7.4 Hz, 2H), 7.56 (dd, J = 6.4, 2.8 Hz, 1H), 7.80 (dd, J = 5.8, 2.6 Hz, 1H), 10.29 (s, 1H). ^{13}C NMR (100 MHz, $CDCl_3$) δ 13.8, 23.2, 30.6 (d, J_{C-F} = 2 Hz), 117.4 (d, J_{C-F} = 4 Hz), 125.4 (d, J_{C-F} = 10 Hz), 128.9 (d, J_{C-F} = 2 Hz), 133.4 (d, J_{C-F} = 18 Hz), 139.5 (d, J_{C-F} = 6 Hz), 162.3 (d, J_{C-F} = 256 Hz), 186.4 (d, J_{C-F} = 8 Hz). LR ESI-LCMS *m*/*z* calculated 245, 247, found 245, 247 $[M+H]^+$.

1-(5-bromo-2-fluoro-3-propylphenyl)ethanone (21k). To a solution of **Y20k** (4.2 g, 17.1 mmol) in ether (50 ml) was added 3 M solution of CH_3MgBr in ether (11.4 ml, 34.3 mmol) at 0 °C. After stirring for 30 min at 0 °C, the reaction was quenched with ice chips and diluted with EtOAc. The organic layer was washed with 1 M HCl aq., sat. $NaHCO_3$ aq. and brine, and then dried and concentrated. The resulting residue was purified by column chromatography on silica gel (hexane-EtOAc gradient) to afford alcohol analogue (4.1 g) of sufficient purity to carry on to the next step. To a solution of the alcohol (4.1 g, 15.7 mmol) in dioxane (50 ml) was added MnO_2 (6.8 g, 78.5 mmol). After stirring for 9 h at 90 °C, the reaction mixture was filtered through celite and concentrated. The resulting residue was purified by column chromatography on silica gel (hexane-EtOAc gradient) to afford **21k** as yellow oil (3.9 g, 15.1 mmol, 88% for 2 steps). ^{1}H NMR (400 MHz, $CDCl_3$) δ 0.94 (t, J = 7.4 Hz, 3H), 1.62 (m, 2H), 2.58-2.62 (m, 4H), 7.44 (dd, J = 6.2, 2.6 Hz, 1H), 7.74 (dd, J = 6.0, 2.8 Hz, 1H). ^{13}C NMR (100 MHz, $CDCl_3$) δ 13.7, 23.1, 30.8 (d, J_{C-F} = 3 Hz), 31.4 (d, J_{C-F} = 8 Hz), 116.8 (d, J_{C-F} = 4 Hz), 127.2 (d, J_{C-F} = 15 Hz), 130.7 (d, J_{C-F} = 3 Hz), 133.2 (d, J_{C-F} = 20 Hz), 137.6 (d, J_{C-F} = 6 Hz), 159.6 (d, J_{C-F} = 253 Hz), 195.0 (d, J_{C-F} = 3 Hz). LR ESI-LCMS *m*/*z* calculated 259, 261, found 259, 261 $[M+H]^+$.

5-bromo-3-methyl-7-propyl-1*H*-indazole (Y1k). To a solution of **Y21k** (2.0 g, 7.72 mmol) in DMF (10 ml) was added hydrazine monohydrate (7.5 ml, 154 mmol). After stirring for 24 h at 120 °C, the reaction was diluted with EtOAc. The organic layer was washed with 1N HCl aq. and then dried and concentrated. The resulting residue was purified by column chromatography on silica gel (hexane-EtOAc gradient) to afford **Y1k** (210 mg, 0.83 mmol, 11%). ^{1}H NMR (400 MHz, $CDCl_3$) δ 1.01 (t, J = 7.4 Hz, 3H), 1.78 (m, 2H), 2.55 (s, 3H), 2.80 (t, J = 7.8 Hz, 3H), 7.26 (s, 1H), 7.67 (s, 1H). ^{13}C NMR (100 MHz, $CDCl_3$) δ 12.3, 14.0, 22.5, 33.3, 113.7, 120.7, 124.3, 126.4, 129.1, 139.6, 143.3. LR ESI-LCMS *m*/*z* calculated 253, 255, found 253, 255 $[M+H]^+$.

5-bromo-2-fluoro-3-*iso*butylbenzaldehyde (Y20l). To a solution of *iso*propyltriphenylphosphonium iodide (25.5 g, 59.1 mmol) in THF (300 ml) was added a 2.5 M solution of *n*-butyllithium in hexane (23.6 ml, 59.1 mmol) at 0 °C. After stirring for 30 min at 0 °C, **Y18** (10.0 g, 49.3 mmol) was added, then the mixture was stirred for 2 h at rt. After removal of the solvent *in vacuo*, the residue was dissolved in EtOAc and filterated on Celite. After concentration of the filtrate, the residue was purified by filtration through a pad of silica gel in a large sintered glass funnel eluting with hexanes to afford styrene analogue (11.7 g). To a solution of the styrene analogue (11.7 g, 51.1 mmol) in THF (450 ml) were added *p*-toluenesulfonyl hydrazide (95.0 g, 511 mmol) and sodium acetate (41.9 g, 511 mmol), and the resulting mixture was stirred at 100 °C for 2 h. After the solvent was removed *in vacuo*, the residue was dissolved in hexane and filtered through a pad of silica gel in a large sintered glass funnel eluting with hexanes. Four times continues treatments with *p*-toluenesulfonyl hydrazide and sodium acetate followed by filtration through silica gel were carried out for reducing styrene completely to yield **Y19l** (8 g). To a solution of **Y19l** (8.0 g) in dry THF was added 2 M solution of LDA in heptanes, THF and ethylbenzene (24.0 ml, 48.5 mmol) at −78 °C and stirred for 1 h at the same temperature. DMF (4.0 ml, 51.9 mmol) was added and the mixture was stirred for additional 1 h at −78 °C. The reaction was quenched with ice chips and diluted with EtOAc. The organic layer was washed with 1 M HClaq. and water, and then dried and concentrated. The resulting residue was purified by column chromatography on silica gel (hexane-EtOAc gradient) to afford **Y20l** (6.0 g, 23.2 mmol, 47% for 3 steps).

^{1}H NMR (400 MHz, $CDCl_3$) δ 0.95 (d, J = 6.8 Hz, 6H), 1.92 (m, 1H), 2.55 (dd, J = 7.2, 1.2 Hz, 2H), 7.53 (dd, J = 6.4, 2.4 Hz, 1H), 7.81 (dd, J = 6.2, 2.2 Hz, 1H), 10.29 (s, 1H). ^{13}C NMR (100 MHz, $CDCl_3$) δ 22.4, 29.4, 37.7 (d, J_{C-F} = 2 Hz), 117.3 (d, J_{C-F} = 4 Hz), 125.4 (d, J_{C-F} = 10 Hz), 129.0 (d, J_{C-F} = 2 Hz), 132.5 (d, J_{C-F} = 17 Hz), 140.1 (d, J_{C-F} = 7 Hz), 162.4 (d, J_{C-F} = 256 Hz), 186.3 (d, J_{C-F} = 8 Hz). LR ESI-LCMS m/z calculated 259, 261, found 259, 261 $[M+H]^+$.

1-(5-bromo-2-fluoro-3-*iso*butylphenyl)ethanone (Y21l). Compound **Y21l** was synthesized from **Y20l** (6.0 g, 23.2 mmol) according to the procedure for **Y21k** by substituting **Y20l** for **Y20k**. Yield: 4.0 g (14.7 mmol, 63% for 2 steps). ^{1}H NMR (400 MHz, $CDCl_3$) δ 0.94 (d, J = 6.8 Hz, 6H), 1.91 (m, 1H), 2.53 (dd, J = 7.2, 1.6 Hz, 2H), 2.62 (d, J = 5.2 Hz, 3H), 7.44 (m, 1H), 7.78 (m, 1H). ^{13}C NMR (100 MHz, $CDCl_3$) δ 22.3, 29.4, 31.5 (d, J_{C-F} = 5 Hz), 38.0 (d, J_{C-F} = 2 Hz), 116.1 (d, J_{C-F} = 4 Hz), 127.3 (d, J_{C-F} = 16 Hz), 130.9 (d, J_{C-F} = 3 Hz), 132.4 (d, J_{C-F} = 20 Hz), 138.4 (d, J_{C-F} = 6 Hz), 159.7 (d, J_{C-F} = 253 Hz), 195.2 (d, J_{C-F} = 3 Hz). LR ESI-LCMS m/z calculated 273, 275, found 273, 275 $[M+H]^+$.

5-bromo-7-isobutyl-3-methyl-1*H*-indazole (Y21l). Compound **Y1l** was synthesized from **Y21l** (4.0 g, 14.7 mmol) according to the procedure for **Y1k** by substituting **Y21l** for **Y21k**. Yield: 160 mg (0.60 mmol, 7%). ^{1}H NMR (400 MHz, $CDCl_3$) δ 0.96 (d, J = 6.8 Hz, 6H), 2.05 (m, 1H), 2.55 (s, 3H), 2.69 (d, J = 7.2 Hz, 2H), 7.23 (s, 1H), 7.67 (s, 1H). ^{13}C NMR (100 MHz, $CDCl_3$) δ 12.2, 22.8, 29.1, 40.8, 113.6, 120.5, 124.3, 125.6, 129.8, 139.9, 143.3. LR ESI-LCMS m/z calculated 267, 269, found 267, 269 $[M+H]^+$.

(*S*)-1-(5-(7-methyl-1*H*-indazol-5-yl)pyridin-3-yloxy)-3-(1*H*-indol-3-yl)propan-2-amine (Y4a). To a solution of stannyl compound **Y2** (200 mg, 0.38 mmol) in DMF (5 ml) were added **Y1a** (120 mg, 0.57 mmol), $Pd_2(dba)_3$ (52 mg, 0.057 mmol), P(*o*-tol)$_3$ (35 mg, 0.11 mmol) and triethylamine (83 μl, 0.57 mmol). After stirring over night at 90 °C, the mixture was diluted with ethyl acetate. The organic layer was washed with water and then dried and concentrated. The resulting residue was purified by column chromatography on silica gel ($CHCl_3$-methanol gradient) to afford **Y3a** (92 mg) of sufficient purity to carry on to the next step. A solution of crude **Y3a** (92 mg) in CH_2Cl_2 (2 ml) and TFA (2 ml) was stirred for 1 h and concentrated. Purification by reversed phase HPLC (gradient of water containing 0.1% TFA-acetonitrile containing 0.1% TFA) followed by lyophilization afforded 2X TFA salt of **Y4a** (40 mg, 0.064 mmol, 17% based on **Y2** for 2 steps). LC Retention 3 : 24. ^{1}H NMR (400 MHz, DMSO-d_6) δ 2.58 (s, 3H), 3.09–3.17 (m, 3H), 3.84 (brs, 1H), 4.17 (m, 1H), 4.34 (m, 1H), 7.00 (t, J = 7.6 Hz, 1H), 7.09 (t, J = 7.4 Hz, 1H), 7.29 (s, 1H), 7.37 (d, J = 8.0 Hz, 1H), 7.48 (s, 1H), 7.62 (d, J = 7.6 Hz, 1H), 7.69 (s, 1H), 7.91 (s, 1H), 8.14 (s, 1H), 8.19 (brs, 2H), 8.31 (s, 1H), 8.58 (s, 1H), 11.03 (s, 1H). HR ESI m/z calculated 398.1975, found 398.1987 $[M+H]^+$.

(*S*)-1-(5-(7-ethyl-1*H*-indazol-5-yl)pyridin-3-yloxy)-3-(1*H*-indol-3-yl)propan-2-amine (Y4b). Compound **Y4b** (2X TFA salt) was synthesized from **Y1b** (64 mg, 0.29 mmol) and **Y2** (100 mg, 0.19 mmol) according to the procedure for **Y4a** by substituting **Y1b** for **Y1a**. Yield: 23 mg (0.036 mmol, 19% based on **Y2** for 2 steps). LC Retention 3 : 30. ^{1}H NMR (400 MHz, DMSO-d_6) δ 1.33 (t, J = 7.6 Hz, 3H), 2.97 (q, J = 7.6 Hz, 2H), 3.09-3.17 (m, 3H), 3.84 (brs, 1H), 4.17 (dd, J = 10.4, 6.0 Hz, 1H), 4.34 (dd, J = 10.6, 3.0 Hz, 1H), 7.00 (t, J = 7.2 Hz, 1H), 7.09 (t, J = 7.4 Hz, 1H), 7.29 (s, 1H), 7.37 (d, J = 8.0 Hz, 1H), 7.47 (s, 1H), 7.62 (d, J = 8.0 Hz, 1H), 7.67 (s, 1H), 7.91 (s, 1H), 8.14 (s, 1H), 8.20 (brs, 2H), 8.30 (s, 1H), 8.58 (s, 1H), 11.03 (s, 1H). HR ESI m/z calculated 412.2131, found 412.2117 $[M+H]^+$.

(*S*)-1-(5-(7-propyl-1*H*-indazol-5-yl)pyridin-3-yloxy)-3-(1*H*-indol-3-yl)propan-2-amine (Y4c). Compound **Y4c** (2X TFA salt) was synthesized from **Y1c** (110 mg, 0.46 mmol) and **Y2** (200 mg, 0.38 mmol) according to the procedure for **Y4a** by substituting **Y1c** for **Y1a**. Yield: 19 mg (0.029 mmol, 7.6% based on **Y2** for 2 steps). LC Retention 3 : 46. ^{1}H NMR (400 MHz, DMSO-d_6) δ 0.96 (t, J = 7.2 Hz, 3H), 1.74 (m, 2H), 2.92 (t, J = 7.4 Hz, 1H), 3.09-3.17 (m, 3H), 3.84 (brs, 1H), 4.17 (dd, J = 10.6, 5.8 Hz, 1H), 4.34 (dd, J = 10.8, 3.2 Hz, 1H), 7.00 (t, J = 7.4 Hz, 1H), 7.09 (t, J = 7.4 Hz, 1H), 7.29 (s, 1H), 7.37 (d, J = 8.4 Hz, 1H), 7.46 (s, 1H), 7.62 (d, J = 8.0 Hz, 1H), 7.66 (s, 1H), 7.91 (s, 1H), 8.13 (s, 1H), 8.20 (brs, 2H), 8.30 (s, 1H), 8.57 (s, 1H), 11.03 (s, 1H). HR ESI m/z calculated 426.2288, found 426.2272 $[M+H]^+$.

(*S*)-1-(5-(7-*iso*butyl-1*H*-indazol-5-yl)pyridin-3-yloxy)-3-(1*H*-indol-3-yl)propan-2-amine (Y4e). Compound **Y4e** (2X TFA salt) was synthesized from **Y1e** (191 mg, 0.75 mmol) and **Y2** (200 mg, 0.38 mmol) according to the procedure for **Y4a** by substituting **Y1e** for **Y1a**. Yield: 28 mg (0.042 mmol, 11% based on **Y2** for 2 steps). LC Retention 3 : 56. ^{1}H NMR (400 MHz, DMSO-d_6) δ 0.93 (d, J = 6.4 Hz, 6H), 2.06 (m, 1H), 2.83 (d, J = 7.2 Hz, 2H), 3.10–3.18 (m, 3H), 3.81 (brs, 1H), 4.25 (dd, J = 10.8, 6.0 Hz, 1H), 4.36 (dd, J = 10.4, 2.8 Hz, 1H), 7.01 (t, J = 7.2 Hz, 1H), 7.10 (t, J = 7.0 Hz, 1H), 7.30 (s, 1H), 7.38 (d, J = 8.0 Hz, 1H), 7.44 (s, 1H), 7.63 (d, J = 7.6 Hz, 1H), 7.70 (s, 1H), 7.93 (s, 1H), 8.14 (s, 1H), 8.20 (brs, 2H), 8.32 (s, 1H), 8.60 (s, 1H), 11.04 (s, 1H). HR ESI m/z calculated 440.2444, found 440.2464 $[M+H]^+$.

(*S*)-1-(5-(7-*n*-pentyl-1*H*-indazol-5-yl)pyridin-3-yloxy)-3-(1*H*-indol-3-yl)propan-2-amine (Y4f). Compound **Y4f** (2X TFA salt) was synthesized from **Y1f** (201 mg, 0.75 mmol) and **Y2** (200 mg, 0.38 mmol) according to the procedure for **Y4a** by substituting **Y1f** for **Y1a**. Yield: 32 mg (0.047 mmol, 12% based on **Y2** for 2 steps). LC Retention 3 : 72. ^{1}H NMR (400 MHz, DMSO-d_6) δ 0.91 (t, J = 7.0 Hz, 3H), 1.39 (m, 4H), 1.77 (m, 2H), 2.99 (t, J = 7.6 Hz, 2H), 3.12-3.22 (m, 3H), 4.23 (dd, J = 10.4, 6.0 Hz, 1H), 4.40 (dd, J = 10.6, 3.0 Hz, 1H), 7.05 (t, J = 7.4 Hz, 1H), 7.14 (t, J = 7.4 Hz, 1H), 7.34 (s, 1H), 7.42 (d, J = 8.4 Hz, 1H), 7.51 (s, 1H), 7.67 (d, J = 7.6 Hz, 1H), 7.74 (s, 1H), 7.96 (s, 1H), 8.18 (s, 1H), 8.24 (brs, 2H), 8.36 (s, 1H), 8.64 (s, 1H), 11.08 (s, 1H). HR ESI m/z calculated 454.2601, found 454.2595 $[M+H]^+$.

(*S*)-1-(5-(7-*iso*-pentyl-1*H*-indazol-5-yl)pyridin-3-yloxy)-3-(1*H*-indol-3-yl)propan-2-amine (Y4g). Compound **Y4g** (2X TFA salt) was synthesized from **Y1g** (201 mg, 0.75 mmol) and **Y2** (200 mg, 0.38 mmol) according to the procedure for

Y4a by substituting **Y1g** for **Y1a**. Yield: 52 mg (0.076 mmol, 20% based on **Y2** for 2 steps). LC Retention 3 : 70. ^{1}H NMR (400 MHz, DMSO-d_6) δ 0.97 (d, J = 6.0 Hz, 6H), 1.63 (m, 3H), 2.96 (t, J = 7.4 Hz, 2H), 3.10-3.18 (m, 3H), 3.85 (brs, 1H), 4.19 (dd, J = 10.8, 6.0 Hz, 1H), 4.36 (dd, J = 10.8, 3.2 Hz, 1H), 7.01 (t, J = 7.0 Hz, 1H), 7.10 (t, J = 7.2 Hz, 1H), 7.30 (s, 1H), 7.38 (d, J = 8.0 Hz, 1H), 7.47 (s, 1H), 7.63 (d, J = 7.6 Hz, 1H), 7.69 (s, 1H), 7.91 (s, 1H), 8.15 (s, 1H), 8.20 (brs, 2H), 8.32 (s, 1H), 8.59 (s, 1H), 11.04 (s, 1H). HR ESI m/z calculated 454.2601, found 454.2620 $[M+H]^+$.

(*S*)-1-(5-(7-phenethyl-1*H*-indazol-5-yl)pyridin-3-yloxy)-3-(1*H*-indol-3-yl)propan-2-amine (Y4h). Compound **Y4h** (2X TFA salt) was synthesized from **Y1h** (230 mg, 0.75 mmol) and **Y2** (200 mg, 0.38 mmol) according to the procedure for **Y4a** by substituting **Y1h** for **Y1a**. Yield: 53 mg (0.074 mmol, 19% based on **Y2** for 2 steps). LC Retention 3 : 70. ^{1}H NMR (400 MHz, DMSO-d_6) δ 3.04 (t, J = 8.2 Hz, 2H), 3.09–3.19 (m, 3H), 3.25 (t, J = 8.2 Hz, 2H), 3.86 (brs, 1H), 4.18 (dd, J = 10.6, 5.8 Hz, 1H), 4.35 (dd, J = 10.6, 3.0 Hz, 1H), 7.01 (t, J = 7.4 Hz, 1H), 7.10 (t, J = 7.2 Hz, 1H), 7.18 (t, J = 7.2 Hz, 1H), 7.27–7.39 (m, 6H), 7.48 (s, 1H), 7.63 (d, J = 7.6 Hz, 1H), 7.66 (s, H), 7.94 (s, 1H), 8.17 (s, 1H), 8.21 (brs, 2H), 8.33 (s, 1H), 8.56 (s, 1H), 11.04 (s, 1H). HR ESI m/z calculated 488.2444, found 488.2438 $[M+H]^+$.

(*S*)-1-(5-(7-chloro-1*H*-indazol-5-yl)pyridin-3-yloxy)-3-(1*H*-indol-3-yl)propan-2-amine (Y4i). Compound **Y4i** (2X TFA salt) was synthesized from **Y1i** (104 mg, 0.45 mmol) and **Y2** (119 mg, 0.22 mmol) according to the procedure for **Y4a** by substituting **Y1h** for **Y1a**. Yield: 39 mg (0.061 mmol, 28% based on **Y2** for 2 steps). LC Retention 3 : 34. ^{1}H NMR (400 MHz, DMSO-d_6) δ 3.08–3.18 (m, 3H), 3.86 (brs, 1H), 4.19 (dd, J = 10.8, 6.0 Hz, 1H), 4.36 (dd, J = 10.6, 3.0 Hz, 1H), 7.01 (t, J = 7.0 Hz, 1H), 7.10 (t, J = 7.2 Hz, 1H), 7.30 (s, 1H), 7.38 (d, J = 8.0 Hz, 1H), 7.63 (d, J = 8.0 Hz, 1H), 7.41 (s, 1H), 7.84 (s, 1H), 8.12 (s, 1H), 8.20 (brs, 2H), 8.29 (s, 1H), 8.35 (s, 1H), 8.62 (s, 1H), 11.03 (s, 1H). HR ESI m/z calculated 418.1429, found 418.1426 $[M+H]^+$.

(*S*)-1-(5-(7-ethyl-3-methyl-1*H*-indazol-5-yl)pyridin-3-yloxy)-3-(1*H*-indol-3-yl)propan-2-amine (Y4j). Compound **Y4j** (2X TFA salt) was synthesized from **Y1j** (94 mg, 0.39 mmol) and **Y2** (200 mg, 0.38 mmol) according to the procedure for **Y4a** by substituting **Y1j** for **Y1a**. Yield: 45 mg (0.069 mmol, 18% based on **Y2** for 2 steps). LC Retention 3 : 42. ^{1}H NMR (400 MHz, DMSO-d_6) δ 1.31 (t, J = 7.6 Hz, 3H), 2.53 (s, 3H), 2.93 (q, J = 7.5 Hz, 2H), 3.06–3.18 (m, 3H), 3.83 (brs, 1H), 4.18 (dd, J = 10.6, 5.8 Hz, 1H), 4.35 (dd, J = 10.6, 3.0 Hz, 1H), 7.00 (t, J = 7.4 Hz, 1H), 7.09 (t, J = 7.6 Hz, 1H), 7.29 (s, 1H), 7.37 (d, J = 8.0 Hz, 1H), 7.46 (s, 1H), 7.62 (d, J = 7.6 Hz, 1H), 7.13 (s, 1H), 7.87 (s, 1H), 8.20 (brs, 2H), 8.31 (s, 1H), 8.62 (s, 1H), 11.03 (s, 1H). HR ESI m/z calculated 426.2288, found 426.2298 $[M+H]^+$.

(*S*)-1-(5-(3-methyl-7-*n*-propyl-1*H*-indazol-5-yl)pyridin-3-yloxy)-3-(1*H*-indol-3-yl)propan-2-amine (Y4k). Compound **Y4k** (2X TFA salt) was synthesized from **Y1k** (100 mg, 0.40 mmol) and **Y2** (116 mg, 0.22 mmol) according to the procedure for **Y4a** by substituting **Y1k** for **Y1a**. Yield: 43 mg (0.064 mmol, 29% based on **Y2** for 2 steps). LC Retention 3 : 48. ^{1}H NMR (400 MHz, DMSO-d_6) δ 1.00 (t, J = 7.4 Hz, 3H), 1.77 (m, 2H), 2.58 (s, 3H), 2.93 (t, J = 7.6 Hz, 2H), 3.16–3.22 (m, 3H), 3.89 (brs, 1H), 4.24 (dd, J = 10.6, 5.8 Hz, 1H), 4.40 (dd, J = 10.4, 2.8 Hz, 1H), 7.05 (1H, t, J = 7.4 Hz, 1H), 7.14 (1H, t, J = 7.2 Hz, 1H), 7.34 (d, J = 2.4 Hz, 1H), 7.42 (d, J = 8.0 Hz, 1H), 7.50 (d, J = 1.2 Hz, 1H), 7.67 (d, J = 8.0 Hz, 1H), 7.79 (t, J = 2.0 Hz, 1H), 7.93 (d, J = 1.6 Hz, 1H), 8.25 (brd, J = 3.2 Hz, 3H), 8.37 (d, J = 2.8 Hz, 1H), 8.37 (d, J = 2.8 Hz, 1H), 8.68 (d, J = 1.6 Hz, 1H), 11.08 (d, J = 2.0 Hz, 1H). ^{13}C NMR (100 MHz, DMSO-d_6) δ 11.7, 13.7, 22.7, 25.0, 32.9, 50.8, 67.6, 107.8, 111.9, 116.1, 117.9, 118.6, 120.0, 120.5, 122.8, 124.8, 125.5, 127.0, 128.0, 135.0, 136.3, 137.8, 140.4, 142.1, 154.7, 158.0, 158.3. HR ESI m/z calculated 440.2444, found 440.2442 $[M+H]^+$.

(*S*)-1-(5-(7-*iso*-butyl-3-methyl-1*H*-indazol-5-yl)pyridin-3-yloxy)-3-(1*H*-indol-3-yl)propan-2-amine (Y4l). Compound **Y4l** (2X TFA salt) was synthesized from **Y1l** (160 mg, 0.60 mmol) and **Y2** (176 mg, 0.33 mmol) according to the procedure for **Y4a** by substituting **Y1l** for **Y1a**. Yield: 55 mg (0.080 mmol, 24% based on **Y2** for 2 steps). LC Retention 3 : 62. ^{1}H NMR (400 MHz, DMSO-d_6) δ 0.87 (d, J = 6.8 Hz, 6H), 2.00 (m, 1H), 2.49 (s, 3H), 2.73 (d, J = 7.2 Hz, 2H), 3.02–3.15 (m, 3H), 3.80 (brs, 1H), 4.14 (m, 1H), 4.29 (dd, J = 22.2, 15 Hz, 1H), 6.96 (t, J = 7.0 Hz, 1H), 7.05 (t, J = 7.6 Hz, 1H), 7.25 (d, J = 2.4 Hz, 1H), 7.33 (d, J = 8.4 Hz, 1H), 7.37 (d, J = 0.8 Hz, 1H), 7.58 (d, J = 8.0 Hz, 1H), 7.64 (s, 1H), 7.83 (d, J = 1.6 Hz, 1H), 8.18 (brs, 3H), 8.26 (d, J = 2.4 Hz, 1H), 8.56 (d, J = 1.2 Hz, 1H), 9.08 (brs, 1H), 11.00 (s, 1H). ^{13}C NMR (100 MHz, DMSO-d_6) δ11.8, 22.3, 25.0, 28.5, 50.7, 67.5, 107.8, 111.6, 116.2, 118.1, 118.6, 119.6, 121.2, 122.8, 124.6, 125.0, 127.0, 128.1, 135.7, 136.3, 137.4, 140.5, 142.0, 154.5, 157.8, 158.1. HR ESI m/z calculated 454.2601, found 454.2579 $[M+H]^+$.

(*S*)-1-(5-(7-butyl-1*H*-indazol-5-yl)pyridin-3-yloxy)-3-(1*H*-indol-3-yl)propan-2-amine (Y4d). To a solution of **Y3i** (170 mg, 0.33 mmol) in toluene (5.5 ml) were added *n*-butylboronic acid (135 mg, 1.33 mmol), $Pd(dba)_2$ (19 mg, 0.033 mmol), 1,2,3,4,5-pentaphenyl-1′-(di-*tert*-butylphosphino)ferrocene (51 mg, 0.066 mmol) and K_3PO_4 (211 mg , 1.0 mmol). After stirring over night at 90 °C, the mixture was diluted with ethyl acetate. The organic layer was washed with water and then dried and concentrated. The resulting residue was purified by reversed phase HPLC (gradient of water containing 0.1% TFA-acetonitrile containing 0.1% TFA) followed by lyophilization afforded the coupling product (10 mg). A solution of the coupling product (10 mg) in CH_2Cl_2 (0.5 ml) and TFA (0.5 ml) was stirred for 1 h and concentrated. Purification by reversed phase HPLC (gradient of water containing 0.1% TFA-acetonitrile containing 0.1% TFA) followed by lyophilization afforded 2X TFA salt of **Y4d** (3.7 mg, 0.0055 mmol, 2% from **Y3i** for 2 steps). LC Retention 3 : 58. ^{1}H NMR (400 MHz, DMSO-d_6) δ 0.93 (t, J = 7.4 Hz, 3H), 1.39 (m, 2H), 1.71 (m, 2H), 2.96 (t, J = 7.6 Hz, 1H), 3.09-3.18 (m, 3H), 3.85 (brs, 1H), 4.19 (dd, J = 10.4, 6.0 Hz, 1H), 4.36 (dd, J = 10.6, 3.0 Hz, 1H), 7.01 (t, J = 7.4 Hz, 1H), 7.10 (t, J = 7.4 Hz, 1H), 7.30 (s, 1H), 7.38 (d, J = 8.0 Hz, 1H), 7.47 (s, 1H), 7.63 (d, J = 8.0 Hz, 1H), 7.70 (s, 1H), 7.92

(s, 1H), 8.14 (s, 1H), 8.20 (brs, 2H), 8.33 (s, 1H), 8.60 (s, 1H), 11.04 (s, 1H). HR ESI m/z calculated 440.2444, found 440.2430 $[M+H]^+$.

References

1 B. D. Manning and L. C. Cantley, *Cell*, 2007, **129**, 1261–1274.
2 A. W. Tolcher, T. A. Yap, I. Fearen, A. Taylor, C. Carpenter, A. T. Brunetto, M. Beeram, K. Papadopoulos, L. Yan and J. de Bono, *J. Clin. Oncol. (Meeting Abstracts)*, 2009, **27**, 3503.
3 D. A. Heerding, N. Rhodes, J. D. Leber, T. J. Clark, R. M. Keenan, L. V. Lafrance, M. Li, I. G. Safonov, D. T. Takata, J. W. Venslavsky, D. S. Yamashita, A. E. Choudhry, R. A. Copeland, Z. Lai, M. D. Schaber, P. J. Tummino, S. L. Strum, E. R. Wood, D. R. Duckett, D. Eberwein, V. B. Knick, T. J. Lansing, R. T. McConnell, S. Zhang, E. A. Minthorn, N. O. Concha, G. L. Warren and R. Kumar, *J. Med. Chem.*, 2008, **51**, 5663–5679.
4 Y. Luo, A. R. Shoemaker, X. Liu, K. W. Woods, S. A. Thomas, R. de Jong, E. K. Han, T. Li, V. S. Stoll, J. A. Powlas, A. Oleksijew, M. J. Mitten, Y. Shi, R. Guan, T. P. McGonigal, V. Klinghofer, E. F. Johnson, J. D. Leverson, J. J. Bouska, M. Mamo, R. A. Smith, E. E. Gramling-Evans, B. A. Zinker, A. K. Mika, P. T. Nguyen, T. Oltersdorf, S. H. Rosenberg, Q. Li and V. L. Giranda, *Mol. Cancer Ther.*, 2005, **4**, 977–986.
5 H. Abeliovich, C. Zhang, W. A. Dunn, Jr., K. M. Shokat and D. J. Klionsky, *Mol. Biol. Cell*, 2003, **14**, 477–490.
6 A. C. Bishop, C.-Y. Kung, K. Shah, L. Witucki, K. M. Shokat and Y. Liu, *J. Am. Chem. Soc.*, 1999, **121**, 627–631.
7 S. T. Eblen, N. V. Kumar, K. Shah, M. J. Henderson, C. K. Watts, K. M. Shokat and M. J. Weber, *J. Biol. Chem.*, 2003, **278**, 14926–14935.
8 A. D. Hindley, S. Park, L. Wang, K. Shah, Y. Wang, X. Hu, K. M. Shokat, W. Kolch, J. M. Sedivy and K. C. Yeung, *FEBS Lett.*, 2004, **556**, 26–34.
9 S. M. Ulrich, D. M. Kenski and K. M. Shokat, *Biochemistry*, 2003, **42**, 7915–7921.
10 B. Dummler and B. A. Hemmings, *Biochem. Soc. Trans.*, 2007, **35**, 231–235.
11 X. Ju, S. Katiyar, C. Wang, M. Liu, X. Jiao, S. Li, J. Zhou, J. Turner, M. P. Lisanti, R. G. Russell, S. C. Mueller, J. Ojeifo, W. S. Chen, N. Hay and R. G. Pestell, *Proc. Natl. Acad. Sci. U. S. A.*, 2007, **104**, 7438–7443.
12 C. W. Lindsley, Z. Zhao, W. H. Leister, R. G. Robinson, S. F. Barnett, D. Defeo-Jones, R. E. Jones, G. D. Hartman, J. R. Huff, H. E. Huber and M. E. Duggan, *Bioorg. Med. Chem. Lett.*, 2005, **15**, 761–764.
13 T. Okuzumi, D. Fiedler, C. Zhang, D. C. Gray, B. Aizenstein, R. Hoffman and K. M. Shokat, *Nat. Chem. Biol.*, 2009, **5**, 484–493.
14 E. K. Han, J. D. Leverson, T. McGonigal, O. J. Shah, K. W. Woods, T. Hunter, V. L. Giranda and Y. Luo, *Oncogene*, 2007, **26**, 5655–5661.
15 A. C. Bishop, J. A. Ubersax, D. T. Petsch, D. P. Matheos, N. S. Gray, J. Blethrow, E. Shimizu, J. Z. Tsien, P. G. Schultz, M. D. Rose, J. L. Wood, D. O. Morgan and K. M. Shokat, *Nature*, 2000, **407**, 395–401.
16 X. Chen, H. Ye, R. Kuruvilla, N. Ramanan, K. W. Scangos, C. Zhang, N. M. Johnson, P. M. England, K. M. Shokat and D. D. Ginty, *Neuron*, 2005, **46**, 13–21.
17 T. Tamguney, C. Zhang, D. Fiedler, K. Shokat and D. Stokoe, *Exp. Cell Res.*, 2008, **314**, 2299–2312.
18 K. W. Woods, J. P. Fischer, A. Claiborne, T. Li, S. A. Thomas, G. D. Zhu, R. B. Diebold, X. Liu, Y. Shi, V. Klinghofer, E. K. Han, R. Guan, S. R. Magnone, E. F. Johnson, J. J. Bouska, A. M. Olson, R. de Jong, T. Oltersdorf, Y. Luo, S. H. Rosenberg, V. L. Giranda and Q. Li, *Bioorg. Med. Chem.*, 2006, **14**, 6832–6846.
19 C. Dell'Erba, M. Novi, G. Petrillo and C. Tavani, *Tetrahedron*, 1994, **50**, 3529–3536.
20 N. Kataoka, Q. Shelby, J. P. Stambuli and J. F. Hartwig, *J. Org. Chem.*, 2002, **67**, 5553–5566.
21 C. Dubost, I. E. MarkÛ and J. Bryans, *Tetrahedron Lett.*, 2005, **46**, 4005–4009.
22 S. Antonysamy, G. Hirst, F. Park, P. Sprengeler, F. Stappenbeck, R. Steensma, M. Wilson and M. Wong, *Bioorg. Med. Chem. Lett.*, 2009, **19**, 279–282.
23 Z. A. Knight and K. M. Shokat, *Chem. Biol.*, 2005, **12**, 621–637.
24 T. G. Davies, M. L. Verdonk, B. Graham, S. Saalau-Bethell, C. C. Hamlett, T. McHardy, I. Collins, M. D. Garrett, P. Workman, S. J. Woodhead, H. Jhoti and D. Barford, *J. Mol. Biol.*, 2007, **367**, 882–894.
25 K. M. Specht and K. M. Shokat, *Curr. Opin. Cell Biol.*, 2002, **14**, 155–159.
26 W. A. Weiss, S. S. Taylor and K. M. Shokat, *Nat. Chem. Biol.*, 2007, **3**, 739–744.
27 Z. A. Knight, M. E. Feldman, A. Balla, T. Balla and K. M. Shokat, *Nat. Protoc.*, 2007, **2**, 2459–2466.
28 L. Zheng, U. Baumann and J. L. Reymond, *Nucleic Acids Res.*, 2004, **32**, e115.

